A BENCHMARKING STUDY OF THE APPLICATION OF A DISTRIBUTED BRAGG REFLECTOR AS BACK-REFLECTOR ON N-PASHA SOLAR CELLS

S.L. Luxembourg[a] , P. Spinelli[a], A. Ingenito[b], J. Liu[a], O. Isabella[b], M. Zeman[b], A.W. Weeber[a,b]
[a]ECN Solar Energy, P.O. Box 1, NL-1755 ZG Petten, the Netherlands - email: luxembourg@ecn.nl
[b]Delft University of Technology, Department of Electrical Sustainable Energy, Mekelweg 4, 2628 CD Delft, the Netherlands

ABSTRACT: A Distributed Bragg Reflector (DBR) optimized for textured substrates was applied as back-reflector to n-Pasha (bifacial) cells. The (infrared) light trapping performance was evaluated and compared to high quality back-reflectors (BRs, *i.e.* Ag, TiO_2) and to a reflective white backsheet (in a single cell laminate). It was found that compared to the open-rear configuration the DBR improves the response to the infrared similar as the other BR options. However, when the cells were combined with a white backsheet in single cell laminates no difference in performance was observed. The ultimate application for a DBR in photovoltaics is thought to be in an ultrathin device in combination with efficient front side trapping. Initial simulations were performed to evaluate and optimize light trapping for a combination of a Mie coating and a DBR. Possible ways for further improvement have been identified.
Keywords: c-Si, bifacial, Light Trapping, n-type, PV module

1 INTRODUCTION

The photonic bandgap of Distributed Bragg Reflector (DBR) structures can be tuned to overlap with the solar cell's spectral range of weak absorption. Therefore, they can potentially be used to improve IR light trapping in solar cells / modules. For the current industry standard of 180 µm thick crystalline silicon (c-Si) solar cells this range corresponds to 1000 to 1200 nm.

On flat substrates DBRs can be designed with close to 100% internal reflection in a range between 800 and 1200 nm [1], thus potentially forming an attractive alternative to metallic Back Reflectors (BRs) to enhance light trapping in PERT and PERC solar cells. Bifacial solar cells can be combined with a reflective backsheet which then acts as a detached BR in a monofacial module configuration. This constitutes another efficient solution for IR light trapping on module level. The latter strategy is employed at ECN in monofacial modules based on n-Pasha solar cells; ECN's bifacial n-type technology with H pattern metallization on both sides [2]. The combination of front-and-rear texture with a reflective backsheet results in efficient IR light trapping on module level.

Recently, at Delft University of Technology a DBR structure was optimized for application to textured Si solar cells [3]. In this study such DBRs were applied as BR on n-Pasha solar cells. The level of IR light trapping was compared to plain n-Pasha cells and to other efficient BR options at the level of cells and in single cell laminates, which included a white backsheet. The other BRs considered in this study are Ag and white paint (WP: TiO_2).

The high reflectivity of DBRs combined with the ability to design them to have omni-directional behavior [1] make them very interesting candidates for any application which requires large optical path length enhancements. In particular, this is the case when moving towards ultrathin Si devices. With a view to this, an initial simulation study was conducted on the use of DBRs as BR in combination with a front (TiO_2) Mie coating for light trapping in an ultrathin (50 µm), flat (non-textured) Si device. Mie coatings can be applied as anti-reflection and light trapping scheme for ultra-thin silicon cells where standard pyramid textures are undesirable as they require removal of significant amounts of Si [4]. Furthermore, they can be applied on polished surfaces in combination with a thin passivation layer to achieve excellent anti-reflection and passivation properties [5].

2 METHODOLOGY

2.1 n-Pasha solar cells

For this study customized n-Pasha c-Si solar cells were fabricated. As the DBRs were deposited onto the solar cells at the Delft University of Technology the n-Pasha platform had to meet the Delft PECVD equipment restrictions. For this purpose, the ECN n-Pasha baseline process flow [2] was followed up to the metallization. 180 µm thick semi-square (156 mm × 156 mm) n-type Cz wafers were front and rear textured followed by boron and phosphorous diffusion to produce the emitter and back surface field, respectively. Subsequently, a-SiN_x:H was deposited on front and rear as anti-reflective coating and passivating layer. The Ag-based metallization grid with metal coverage area of approximately 5% was screen printed and stencilled to the front and rear of the cell in a 10 cm × 10 cm area only. For this purpose custom screens and stencils were used, which resulted for both front and rear in a 45 fingers and three busbars configuration. In addition, the front and rear metallization was aligned, which facilitated measurements in between the fingers. Subsequently, the area of the processed wafer outside of the metal grid was removed through laser scribing and subsequent cleaving. For ease of fabrication all BR options (see below) were applied on top of the rear metallization. To facilitate electrical contacting of the cells, a mask was used during BR application, which prevented total coverage of the busbars by the BRs (Fig. 1).

2.2 Application of back-reflectors

The DBR was applied at Delft University of Technology using an Electrorava PECVD cluster tool. A DBR consists of alternating layers of a high and low refractive index material. The stack applied in this study consisted of a-Si:H and a-SiN_x:H and was optimized for textured surfaces. To enhance its performance, a layer of SiO_2 is deposited using PECVD, prior to the actual DBR [1].

For the Ag BR cells a 100 nm thick Ag layer was applied through PVD. The rear a-SiN_x:H layer of these cells was optimized to prevent plasmonic losses [6]. A thickness of 140 nm was found to be optimal.

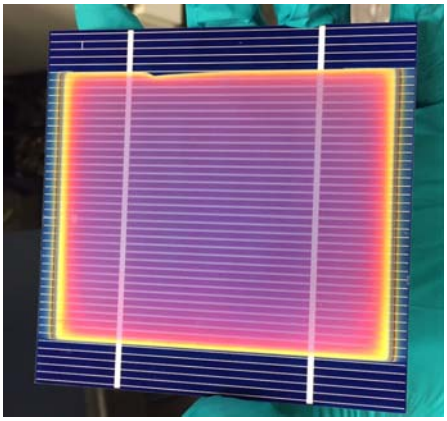

Fig. 1: The DBR applied to the rear of a 10 cm × 10 cm n-Pasha solar cell. The outer edge of the cell was masked during deposition to facilitate contacting of the busbars.

The WP BR was applied through drop-casting of TiO_2 particles mixed in H_2O in a 1:10 ratio followed by drying in air for 12 hours. A minimum thickness of 50 µm was found to be sufficient to ensure transmission below 5% at 1200 nm.

2.3 Single cell laminates

Single cell laminates were prepared from the n-Pasha cells with or without the additional BRs. The cells were encapsulated in a glass – EVA – backsheet stack. The thickness of the glass used, was 3 mm, while front and rear EVA were both 450-µm thick. A white reflective backsheet was used with a reflection in the IR range of approximately 85%.

2.4 Measurement methodology

J-V measurements were performed on a Wacom AAA solar simulator. No correction for spectral mismatch was performed. The cells were measured on a brass reflective measurement chuck, which is normally used in our measurements of bifacial cells (simulating the backsheet in conventional monofacial modules). In addition, we used a measurement chuck on which we applied a black foil with low IR reflectivity (~3%). With the latter approach we were able to isolate the contribution of the additional on-cell BR, while in the measurements with the brass chuck the bifacial cells benefit from the IR reflection of the chuck. The single cell laminates were measured on the same system.

Spectral Response measurements were performed both at Delft University of Technology and at ECN. The Delft set-up was used to perform local measurements in-between the fingers of the solar cells. These measurements were performed in air, with no reflective backing. At ECN the single cell laminates were measured using a full area spectral response (SR) set-up. From the SR data the External Quantum Efficiency (EQE) was calculated.

2.5 Ultrathin Si simulations

Numerical simulations were performed using S4 software developed by Stanford University [7]. For each configuration the absorption spectrum was simulated in a spectral range of 300-1200 nm. The total photogenerated current density (J_{ph}) was then calculated by integrating the absorption spectrum over the spectral range by weighting with the AM1.5 photon flux solar spectrum.

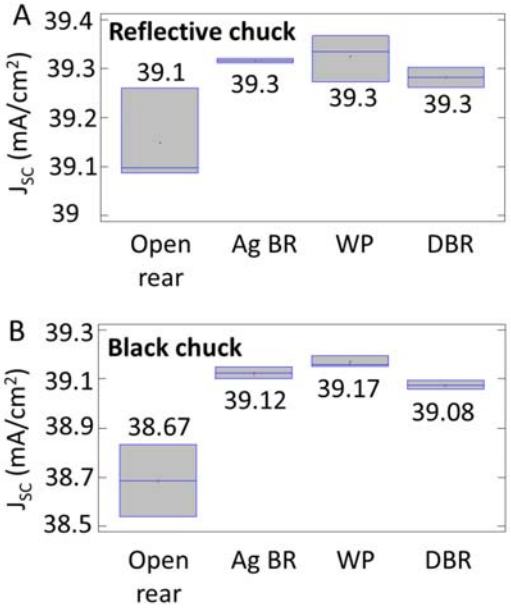

Fig. 2: A) J_{sc} of the different BR configurations recorded on the brass, reflective chuck and **B**) on the non- reflective chuck.

3 RESULTS

3.1 DBR applied in n-Pasha cells and modules

In Fig. 2A the J_{sc} values recorded in the J-V measurements using the reflective chuck are reported. From this figure a modest gain for the cells with on-cell BR is observed. To be able to isolate the effect of the BRs the measurements were repeated with a chuck covered with black foil. In this case the bifacial cells no longer benefit from the brass chuck reflection. As can be seen in Fig. 2B the difference in recorded J_{sc} between the bifacial n-Pasha cell and cells with additional BR is now increased to approximately 0.5 mA/cm^2. No significant difference between the different BR configurations was recorded. As expected, fill factor and V_{oc} did not differ among the different cells. As a consequence of the measurement methodology the measured J_{sc} for the cells equipped with on-cell BRs is approximately 0.2 mA/cm^2 higher on the reflective chuck. As the cells do not cover the entire measurement chuck, in the measurement on the reflective chuck, part of the chuck is left unshielded. As a result light reflected from this area is partly added to (the diffuse component) of the incident light.

In Fig. 3 the EQE curves of the cells with the different BR configurations are shown. Clearly, the EQE data confirm that the differences in J_{sc} found above result from improved IR light absorption with the on-cell BRs present.

Similar measurements were performed for the laminated cells, these are included in Fig. 4A and B. The EQE in this case was measured with full area illumination. From these results it follows that when a highly reflective white backsheet is included as external back-reflector, there is no significant difference in J_{sc} between the open-rear and BR configurations. This finding is confirmed in the EQE curves, which overlap in the NIR range.

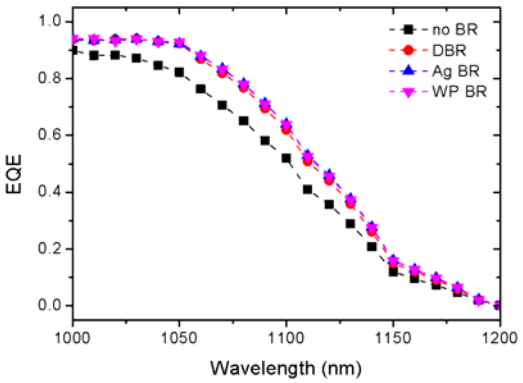

Figure 3: A comparison of the EQE curves measured for the cells equipped with the different BR configurations

3.2 Simulation of an ultrathin Si device

The simulated structure is shown in Fig. 5A. The parameters for a DBR structure optimized for application on a flat Si device were taken from [1]. A first coarse optimization of the TiO_2 Mie coating was performed. As starting point the optimal geometry for thick wafers, optimized for anti-reflection, was used (350 nm diameter and 100 nm height) [5]. Subsequently, the Mie coating geometry was optimized by changing the TiO_2 nanoparticle diameter between 300 nm and 400 nm and the height between 50 and 150 nm.The distance between the nanoparticles was fixed to 500 nm, that is an optimal value for AR properties. Note that this parameter is more important for thinner devices (< 10-µm thick), where coupling to waveguide modes via scattering from the grating is the main mechanism for light trapping. Table I shows J_{ph} for all configurations. As can be seen, the optimal geometry that was found for thick wafers is also the best for a 50-µm thick silicon slab. A total J_{ph} of 36.9 mA/cm^2 was calculated for the optimal geometry.

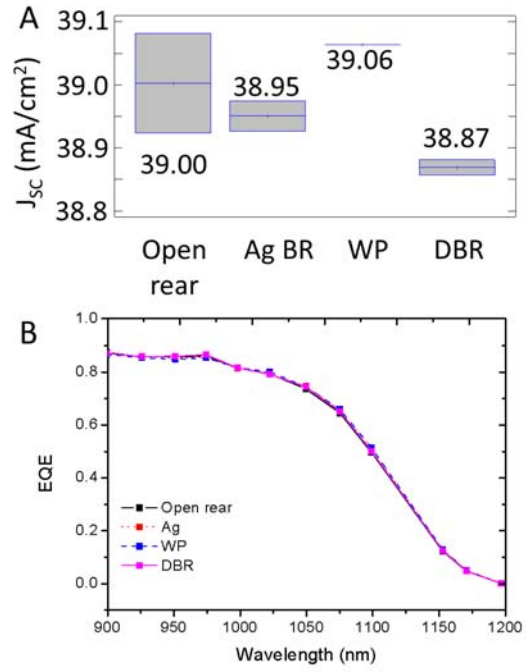

Figure 4: A) J_{sc} determined from J-V measurements on single cell laminates (including a white backsheet) of the cells with different BR configurations. **B**) NIR range of the EQE curves recorded for the same single cell laminates.

Table I: Simulated J_{ph}, the column labeled with minus (plus) corresponds to low (high) values for the height and diameter of the pillars.

J_{ph} (mA/cm^2)	-	Optimal	+
Height	35.0	36.9	36.8
Diameter	36.8	36.9	36.3

The absorption of a 50-µm thick Si slab with front Mie coating and DBR rear reflector was compared with its absorption in the case of the $4n^2$ limit (see Fig. 5B). The $4n^2$ absorption limit was calculated using the generalized formula developed by Green in ref. [8]. The graph also shows the double pass (dashed) absorption for a 50-µm Si layer. As can be seen, the Si absorption with the Mie coating follows that of double pass absorption. This suggests that, while the current structure provides excellent, broadband front side anti-reflection and rear side reflection, the light scattering effect in the IR spectral range still has to be optimized.

In order to improve the light trapping effect, three ways are suggested:

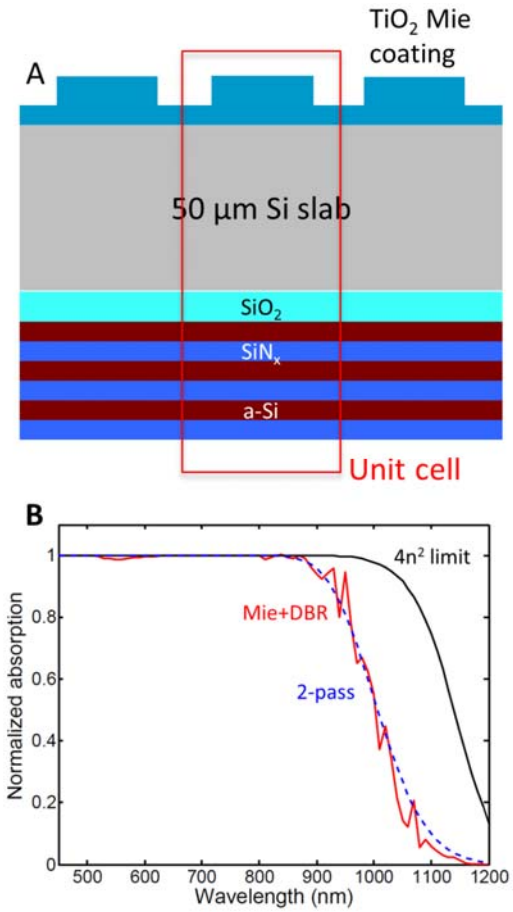

Figure 5: A) Simulated structure with the unit cell indicated. **B**) Normalized absorption in the Si slab compared to the $4n^2$ and 2-pass situations.

1. Increase the index of TiO_2 by e.g. post deposition annealing or by sputter deposition
2. Randomize the position of TiO_2 nanoparticles
3. Include an additional degree of scattering at the rear through texturing [1].

A high index nanoparticle material is favorable because of better index match between nanoparticles and substrate allow for a stronger scattering effect towards the substrate. Different light trapping schemes based on higher refractive index Si nanostructures have been shown to yield absorption that are above 80% of the $4n^2$ limit [1,9,10]. In the best case, 98% of the $4n^2$ limit was achieved over a broad spectral range. Furthermore, all these results were realized using randomized or semi-randomized configurations of nanostructures. Randomization has been shown to substantially improve the absorption of light into a thin layer of material [10].

4 DISCUSSION AND CONCLUSIONS

In this benchmarking study we have shown that a DBR optimized for textured substrates behaves as very efficient back-reflector. On cell level, internal reflection similar to other high quality BR options like silver is achieved. Thereby, it is a metal-free alternative option as on-cell BR. Nevertheless, in a module the combination of a bifacial cell with a (cheap) and highly reflective backsheet results in very similar NIR response and overall J_{sc} as achieved with the on-cell BR options. The NIR internal reflection which can be achieved with the DBR on textured substrates is not sufficient to improve NIR absorption over the level obtained with the bifacial cell – white backsheet combination. As detailed in [3] this is most likely caused by the non-conformal growth around the tip and valleys of the pyramid texture. Therefore, the application of a DBR as BR on flat surfaces is considered more promising. Still, even for a textured rear the application of a DBR does remove the necessity to combine an open-rear cell with a highly reflective backsheet on module level, which increases freedom of module design, allowing for combination with black, colored or transparent backsheets.

Another obvious application of DBRs is the application in an ultrathin device. The combination with a front Mie coating studied here shows excellent light in-coupling and rear side reflection but needs further optimization and/or synergy with other light management approaches to improve IR absorption through scattering / diffraction.

This work was carried with a subsidy from the Dutch Ministry of Economic Affairs under the EOS-LT program (Project No. EOSLT10037). The authors would like to acknowledge Martijn Ronchetti and Eric Kossen (ECN) for the design of the metallization screens and stencils used in this study.

5 REFERENCES

[1] A. Ingenito, O. Isabella, M. Zeman, *Experimental Demonstration of 4n2 Classical Absorption Limit in Nanotextured Ultrathin Solar Cells with Dielectric Omnidirectional Back Reflector*, ACS Photonics **1**, 270 (2014)

[2] I. G. Romijn, G. Janssen, M. Koppes, J. Liu, Y. Komatsu, J. Anker, A. Gutjahr, E. Kossen, A. Mewe, K.. Tool, O. Siarheyeva, M. Ernst, *Towards 21%: front side improvements for n-Pasha solar cells*, Proceedings of SNEC 8th International Photovoltaic Power Generation Conference & Exhibition, Shanghai, China (2014).

[3] A .Ingenito, S.L .Luxembourg, P. Spinelli, J. Liu, J.C. Ortiz Lizcano, A.W. Weeber, O. Isabella, M. Zeman, *Optimized metal-free back reflectors for high efficiency open rear c-Si solar cells*, IEEE J. Photovolt., accepted for publication (2015).

[4] P. Spinelli, M.A. Verschuuren, and A. Polman, *Broadband omnidirectional antireflection coating based on subwavelength surface Mie resonators*, Nature Comm. **3**, 692 (2012)

[5] P. Spinelli, B. Macco, M. A. Verschuuren, W.M.M. Kessels, and A. Polman, *Al2O3/TiO2 nano-pattern antireflection coating with ultralow surface recombination,* Appl. Phys. Lett. **102**, 233902 (2013)

[6] Z. C. Holman, M. Filipič, B. Lipovšek, S. De Wolf, F. Smole, M. Topič, C. Ballif, *Parasitic absorption in the rear reflector of a silicon solar cell: Simulation and measurement of the sub-bandgap reflectance for common dielectric/metal reflectors*, Sol. Energ. Mat. Sol. **120**, 426 (2014).

[7] V. Liu and S. Fan, *S4: A free electromagnetic solver for layered periodic structures*, Computer Physics Communications 183, 2233-2244 (2012)

[8] M.A. Green, *Lambertian light trapping in textured solar cells and light-emitting diodes: analytical solutions*, Progress in Photovoltaics **10**, 235-241 (2002)

[9] P. Spinelli, *Light trapping in solar cells using resonant nanostructures*, PhD thesis, University of Amsterdam (2013)

[10] E. R. Martins, J. Li, Y. Liu, V. Depauw, Z. Chen, J. Zhou, and T. F. Krauss, *Deterministic quasi-random nanostructures for photon control*, Nature Comm. **4**, 2665 (2013)